Nanosecond pulsed laser generation of holographic structures on metals

Krystian L. Wlodarczyk*[a], Marcus Ardron[b], Nick J. Weston[b], Duncan P. Hand[a]
[a]Institute of Photonics and Quantum Sciences, School of Engineering and Physical Sciences, Heriot-Watt University, Edinburgh, EH14 4AS, United Kingdom;
[b]Renishaw plc, Research Park North, Riccarton, Edinburgh, EH14 4AP, United Kingdom

ABSTRACT

A laser-based process for the generation of phase holographic structures directly onto the surface of metals is presented. This process uses 35ns long laser pulses of wavelength 355nm to generate optically-smooth surface deformations on a metal. The laser-induced surface deformations (LISDs) are produced by either localized laser melting or the combination of melting and evaporation. The geometry (shape and dimension) of the LISDs depends on the laser processing parameters, in particular the pulse energy, as well as on the chemical composition of a metal. In this paper, we explain the mechanism of the LISDs formation on various metals, such as stainless steel, pure nickel and nickel-chromium Inconel® alloys. In addition, we provide information about the design and fabrication process of the phase holographic structures and demonstrate their use as robust markings for the identification and traceability of high value metal goods.

Keywords: Laser marking, diffractive optics, holograms, surface modification

1. INTRODUCTION

Many goods, including electronics, jewelry, automotive and aviation parts, must be marked following the manufacturing process in order to provide their full identification and traceability. Common approaches to marking include etching of serial numbers, barcodes, 2D codes or the use of polymer holographic stickers that are typically produced by a mechanical embossing process. All these markings, however, can be easily damaged and tampered, and hence they are vulnerable to counterfeiting. Moreover, the holographic stickers are only attached as an adhesive tape, so that they can be easily removed.

In this work, we are focusing on the development of a laser-based process for the generation of unique phase holographic structures with micro-sized features (called pixels) directly on the surface of metals, making them tamperproof. Lasers are increasingly used in many industrial sectors, including automotive, aerospace and electronics, for cutting, drilling, marking, and welding as well as for surface polishing and smoothing. In these last two processes, the laser beam is used to generate a melt pool on the work piece surface, enabling the molten layer to flow under surface tension forces, thereby causing surface relaxation and consequently surface roughness reduction [1]. Typically, however, new surface deformations such as bumps, dimples, corrugations and ripples are also generated during the re-melting and re-solidification process. As explained in [2-4], the shape and dimensions of these deformations depend on the absorbed laser intensity, maximum temperature and temperature gradients generated in the molten layer, as well as the chemical composition of the materials.

This paper presents a laser-based process for the generation of unique, optically-smooth, phase holographic structures directly on the surface of different metals, such as stainless steel, pure nickel and nickel-chromium Inconel® alloys. The optical smoothness of the holograms is obtained by using nanosecond laser pulses of wavelength 355nm. As reported elsewhere [5], UV nanosecond laser pulses are very suitable for structuring the surface of various metals, e.g. stainless steel. They generate a very shallow melt pool with a transverse thermal gradient since the laser beam is more intense in the center. This gives rise to a surface tension gradient across the surface of the melt pool, causing a flow of the molten material, known as the Marangoni effect [4], and the formation of optically-smooth surface features. Therefore, in this work UV nanosecond laser pulses are used to sculpt a metal in order to generate phase holograms that can act as robust markings for the identification and traceability of high value metal products and components, using either melting or the combination of melting and evaporation.

*K.L.Wlodarczyk@hw.ac.uk; phone +44 (0) 131 451 3105; fax +44 (0) 131 451 4155.

In this work, we are interested in the generation of very shallow craters with well-controlled depths of up to 200nm in order to construct either a binary or multi-level phase hologram with a high diffraction efficiency. Based on diffractive optics theory [6], the highest diffractive efficiency for a reflective binary hologram is obtained when the depth of pixels corresponds to a quarter of the laser wavelength (λ/4) used for reading the phase diffractive optical element (DOE) – this is valid for the 'ideal' reflective DOEs (with a flat, optically-smooth base).

2. LASER SET-UP

The experimental setup used in this work is shown in Figure 1. The setup is based on a 10W Q-switched diode-pumped laser (JDSU Q-series) that provides 35ns long pulses of a nominal wavelength 355nm. The laser beam is delivered to the work piece via a half-wave (λ/2) plate, polarizing beam splitter (PBS), a ×3 beam expander (BEX), a 2-axis beam deflection unit (galvo scan head), and a flat-field (F-theta) lens with a focal length of 108mm. The diameter of the laser spot on the work piece was measured to be 11±2.2μm (at $1/e^2$ of its maximum intensity).

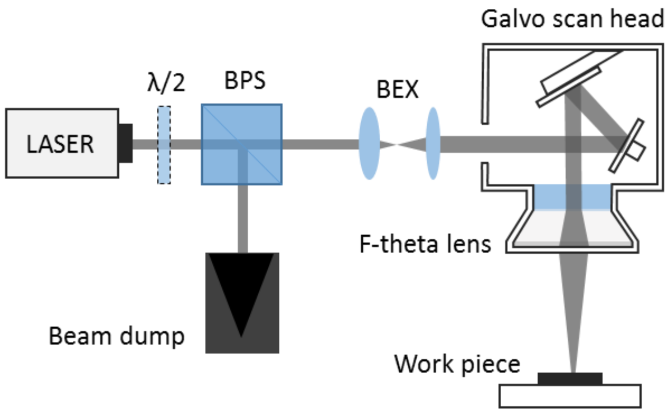

Figure 1. Laser setup used for the generation of phase holographic structures.

Rough adjustment of the maximum laser power (pulse energy) delivered to the work piece is achieved by rotating the λ/2 plate, whereas fine control of the laser power (pulse energy) is carried out using an arbitrary waveform generator (AWG) that modulates and triggers the laser. The galvo scan head is combined with the laser in such way that laser pulses are delivered on demand to a certain location on the work piece, so called the 'point & shoot' operation. The galvo scan head is controlled by Raylase weldMARK 3 software.

3. INTERACTION OF UV NANOSECOND LASER PULSES WITH SELECTED METALS

We investigated the interaction of UV nanosecond laser pulses with different metals such as stainless steel, pure nickel, silver, Inconel®625, and Inconel®718 alloys. The surface of the metal samples was lapped and polished before laser treatment. The metal samples had different thicknesses in the range of 0.18-2.0mm.

Figure 2 shows an example of a calibration map that was generated on the surface of Inconel®718 alloy. In this case, the laser set-up was adjusted in such way that the maximum pulse energy delivered to the work piece was only 15μJ. As can be seen in Fig. 2, the calibration map contains a large quantity of small laser machined areas; each having an array of laser-induced surface deformations (LISDs) that were created by single laser pulses at a constant pulse energy (E_P in the range of 0.45 to 13.8μJ). The same calibration procedure was carried out also for the other metals samples, i.e. stainless steel, pure nickel, silver, and Inconel®625 alloy.

A detailed analysis of the calibration maps was performed using an optical microscope (Leica) and an atomic force microscope (Digital Instruments Veeco). The AFM enabled accurate measurement of the shape and dimension (depth and diameter) of the LISDs, with a lateral (spatial) resolution of <0.2μm and a vertical resolution of ≤1nm.

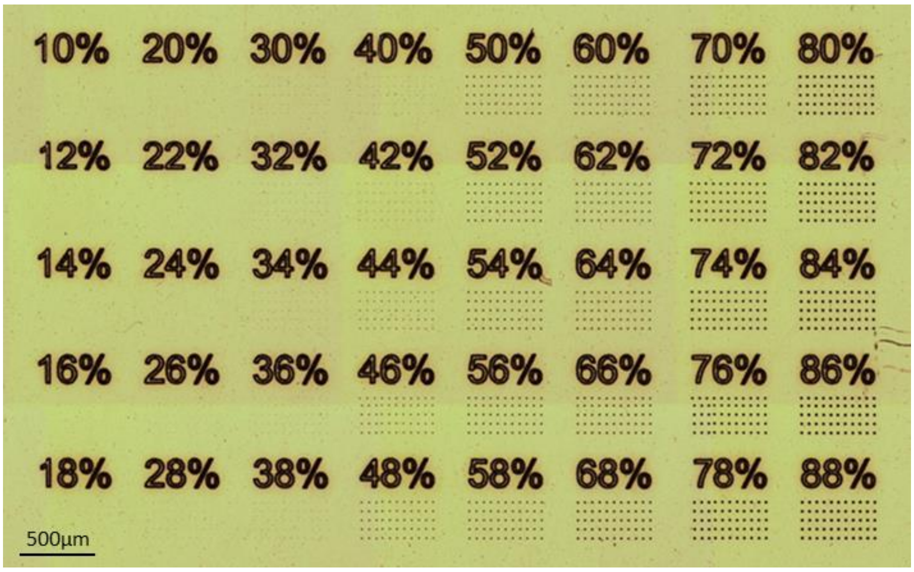

Figure 2. An optical microscope image of the calibration map performed on Inconel®718 alloy.

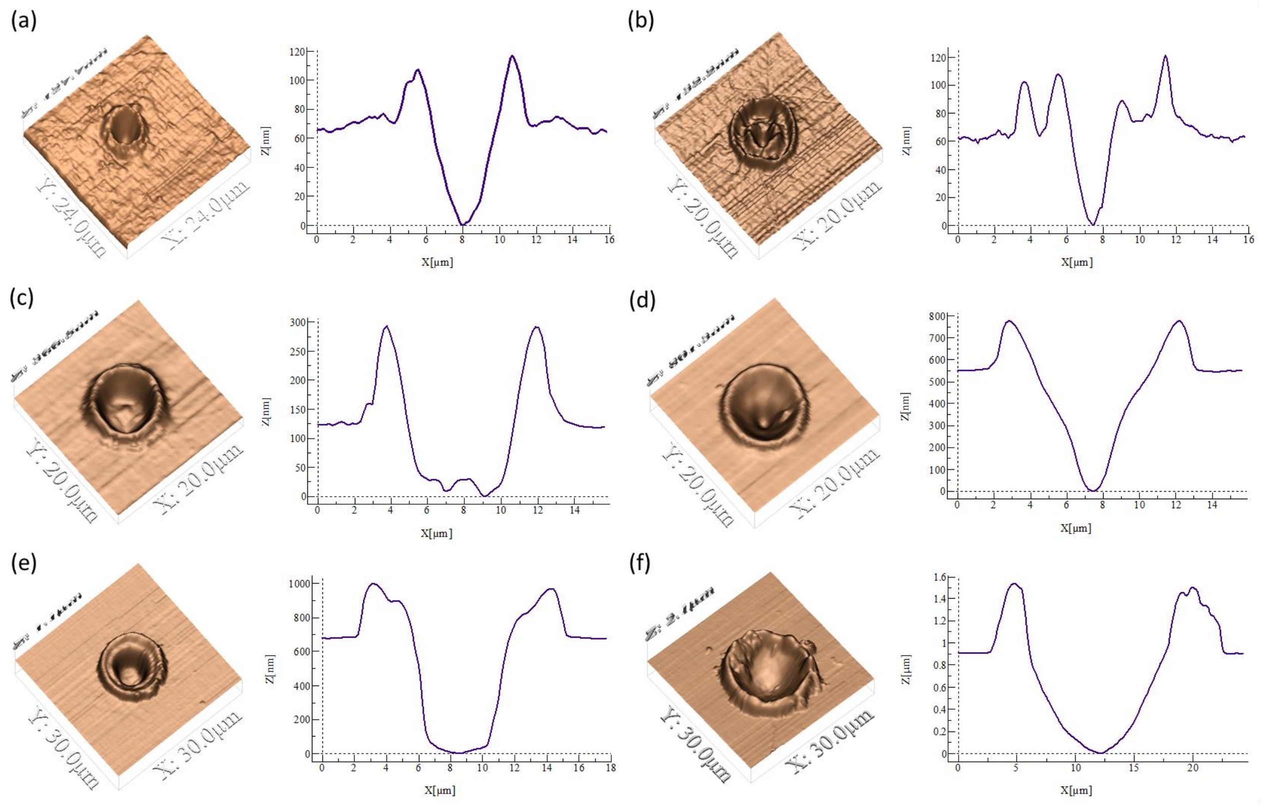

Figure 3. Example of the LISDs generated on the surface of stainless steel. The deformations were produced by single laser pulses with a pulse energy of: (a) 2.6µJ, (b) 4.0µJ, (c) 6.2µJ, (d) 7.2µJ, (e) 8.5µJ and (f) 13.5µJ.

Figure 3 shows examples of the LISDs obtained on the surface of stainless steel. Just above the pulse energy at which the LISDs were detectable by the AFM, i.e., near the threshold ($E_P \approx 2\mu J$), the deformations were observed as shallow and optically-smooth craters with a depth not exceeding 100nm (see Fig. 3(a)). For slightly higher pulse energies (up to

5.2µJ), these craters were surrounded by a rim, as can be seen in Fig. 3(b). For pulse energies between 4.5 and 6.9µJ, the deformations had a shape of optically-smooth craters with a relatively flat base, as shown in Fig. 3(c). The depth of these craters never exceeded 300nm, and hence such craters can be used for the generation of phase holographic structures. For pulse energies above 6.9µJ, the craters become deeper than 0.5µm, mainly due to the appearance of a "keyhole" (analogous to that observed with laser welding processes) that can be seen in Fig. 3(d). This keyhole becomes wider with increasing pulse energy, as shown in Fig. 3(e). For pulse energies above 10.9µJ (see Fig. 3(f)), the keyhole disappeared; instead the LISDs were surrounded by re-solidified splashes of the molten metal.

Similar analysis of the LISDs was carried out for the other metal samples (not included in this work) in order to determine the range of pulse energy that is appropriate for the generation of shallow and optically-smooth craters which later can be used for the manufacture of phase holographic structures.

Figures 4 and 5 show the depth and diameter of the LISDs measured for all five metal samples. Figure 4 presents the results obtained for stainless steel, nickel and silver, whereas Figure 5 shows the results for the Inconel® alloys.

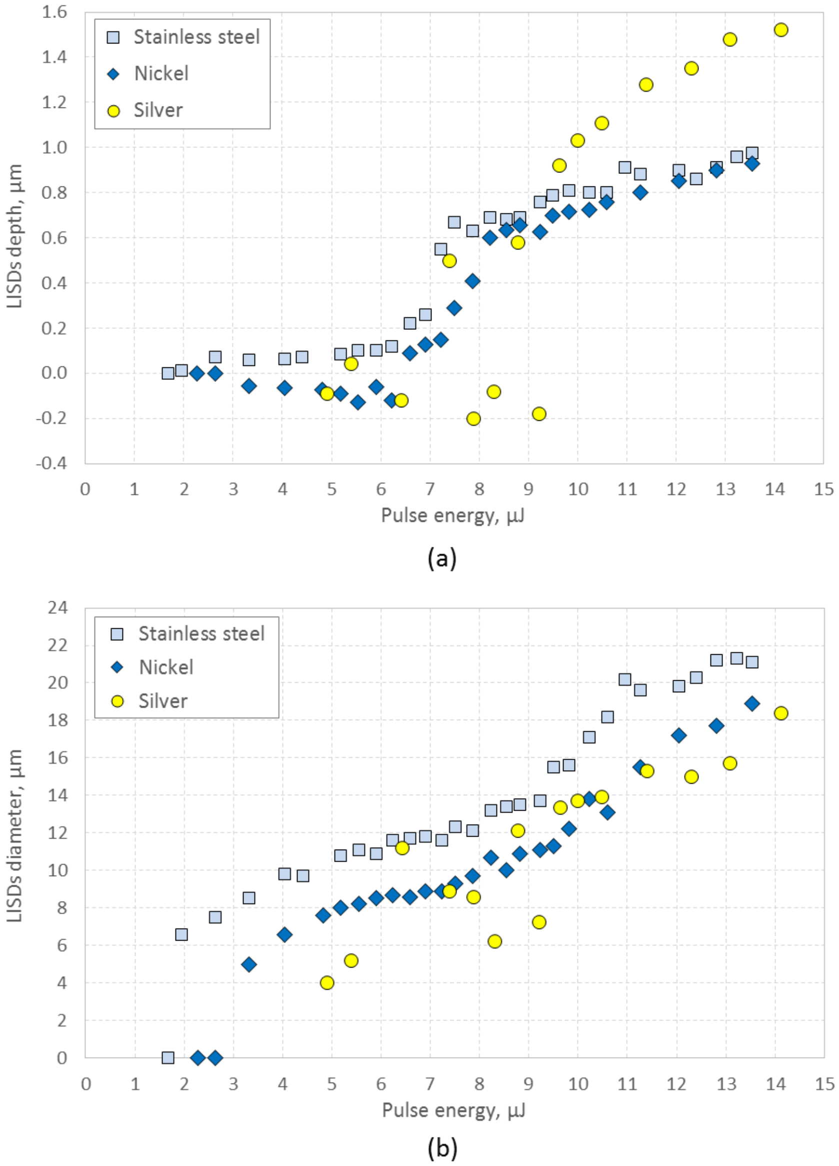

Figure 4. (a) Depth and (b) diameter of the LISDs generated on the surface of stainless steel, nickel and silver.

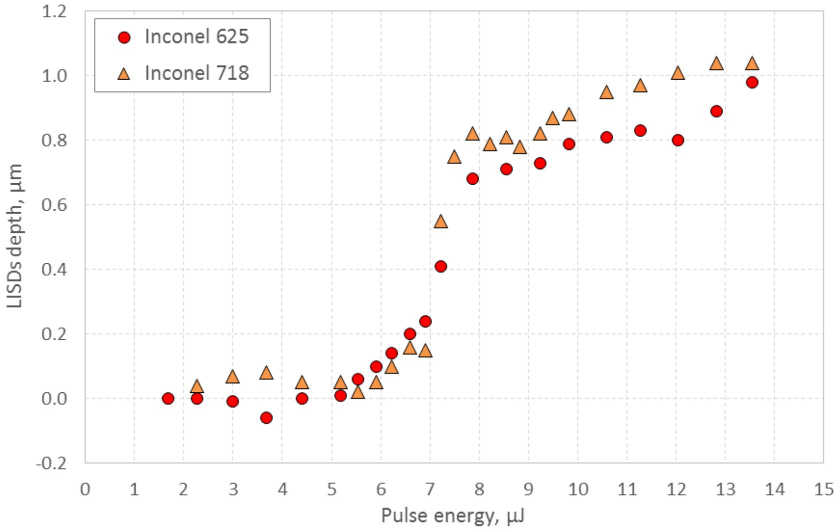

(a)

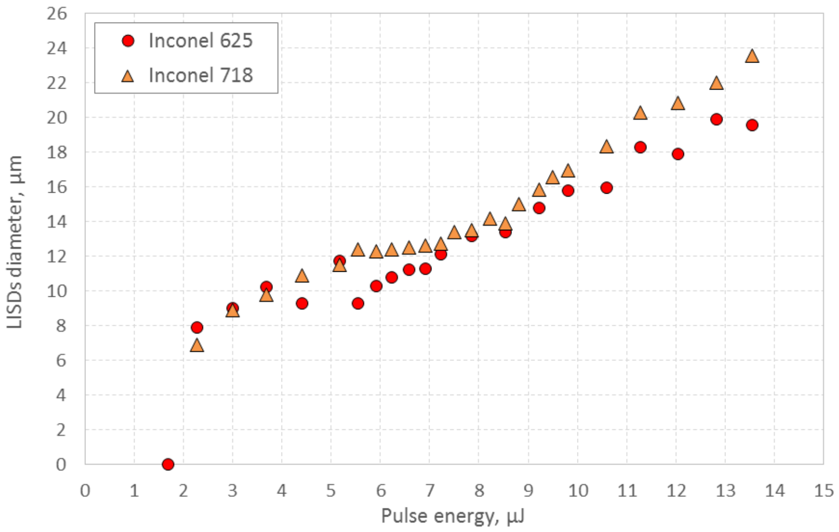

(b)

Figure 5. (a) Depth and (b) diameter of the LISDs generated on the surface of Inconel® alloys.

Of the metals tested, only silver did not provide satisfactory results, i.e. in this case it was not possible to obtain a depth of the LISDs (craters) in the range of 0 to 200nm. As can be seen in Fig. 4, the depth and diameter vary significantly with a small increase of the pulse energy. This is related to the fact that silver has a very high reflectivity (R > 65%) at the wavelength of 355nm. Moreover, this reflectivity is highly temperature-dependent; hence the absorptivity is in effect highly nonlinear with laser pulse energy, resulting in a wide variation of shapes for nominally identical pulse energy. This is clearly shown in the optical microscope image in Fig. 6 that includes LISDs generated with a constant pulse energy on: (a) pure nickel and (b) silver. Hence, it can be concluded that UV nanosecond laser pulses cannot be used for sculpting the silver, but can be used for sculpting the other metals.

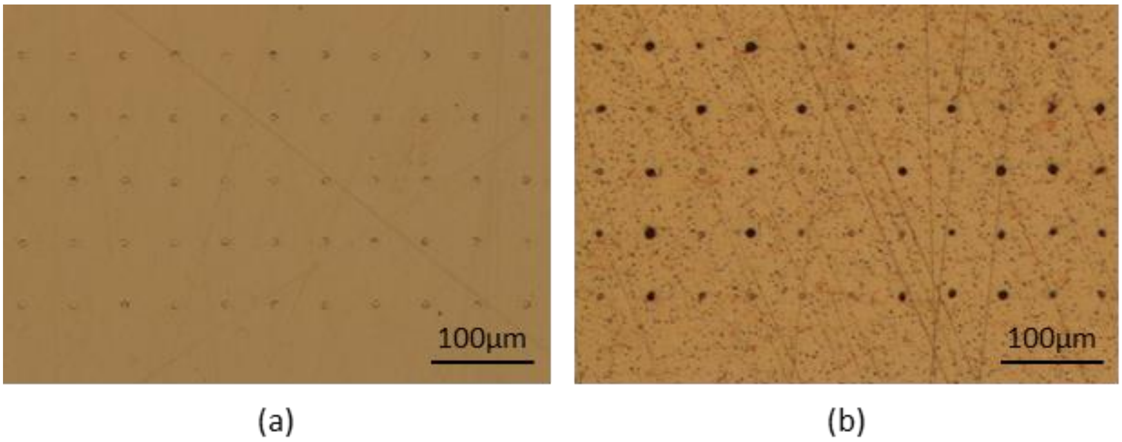

Figure 6. Optical microscope image of craters generated near the laser-induced surface threshold on: (a) pure nickel at E_P = 6.6µJ and (b) silver at E_P = 8.8µJ

4. GENERATION OF PHASE HOLOGRAPHIC STRUCTURES

The design and fabrication process of the phase holographic structures on the surface of metals is presented in Fig. 7. This can be explained as follows:

a) Information in the form of an image and/or alphanumeric characters that will be produced by a hologram is designed using a simple graphical tool (e.g. MS Paint). The image design must be saved as a 'mirror' image because it will be generated by a hologram written on a metal (reflective) surface.

b) An image design is processed using the Iterative Fourier Transform Algorithm (IFTA) in order to generate a single period of the hologram design (also called a Computer Generated Hologram). The IFTA enables the generation of two-level (binary) and multi-level CGHs.

c) To increase an effective aperture of the holographic structure, the designed CGH is often copied several times and tiled in an '$m \times n$' arrangement.

d) The tiled hologram design is mapped onto the surface of a metal work piece using a focused UV laser beam.

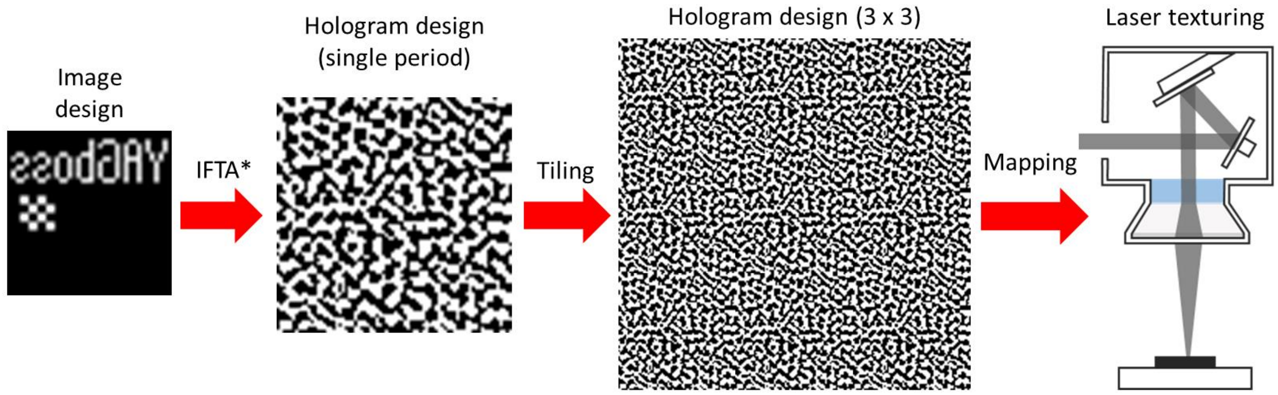

Figure 7. Design and fabrication process of holographic structures on metals.

An example of the holographic structure that was generated on the surface of stainless steel is shown in Fig. 8. This structure contains 228 × 228 pixels. Black areas in the hologram design (see Fig. 7) represent optically-smooth craters with a typical depth of < 250nm. The overall dimension of the hologram shown in Fig. 8 is approximately 1.6 × 1.6mm. Our laser marking system presented in Section 2 enables the generation of such holograms in the time of less than a minute.

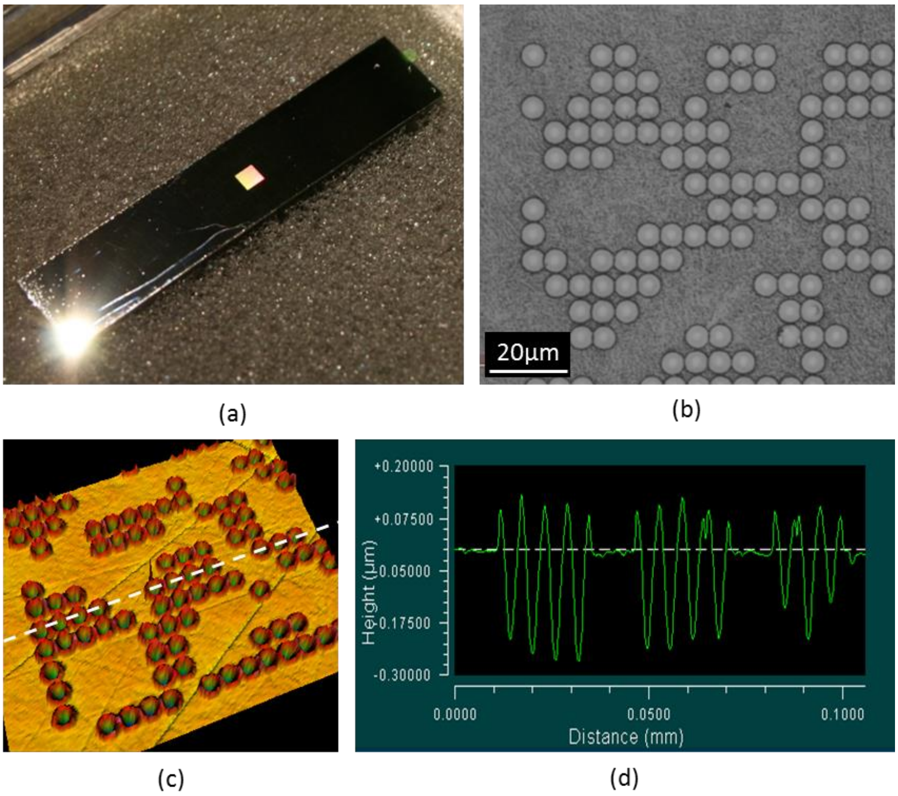

Figure 8. Example of a binary holographic structure generated on stainless steel: (a) photograph, (b) optical microscope image of selected area of the structure, (c) 3D surface profile and (d) cross-section of the hologram pixels. Source: [7].

An optical setup that can be used for 'reading' the laser-generated holograms is shown in Fig. 9(a). In this setup, the red beam ($\lambda \approx 650$nm) from a low-cost laser pointer is used to illuminate the holographic structure in order to generate a diffractive image onto a screen in the far field. Typically, the screen must be located at least 1 meter away from the hologram. Figure 9(b) shows the diffractive image generated by the two-level holographic structure shown in Fig. 8. The hologram produces the 'YAGboss' inscription and a checkerboard pattern, making them consistent with the image design from Fig. 7, but it also contains the undiffracted 0^{th} order beam and the second 'twin' image that is rotated with respect to the other by 180 degrees. The appearance of the 'twin' image is a consequence of the hologram having only 2 phase levels [8].

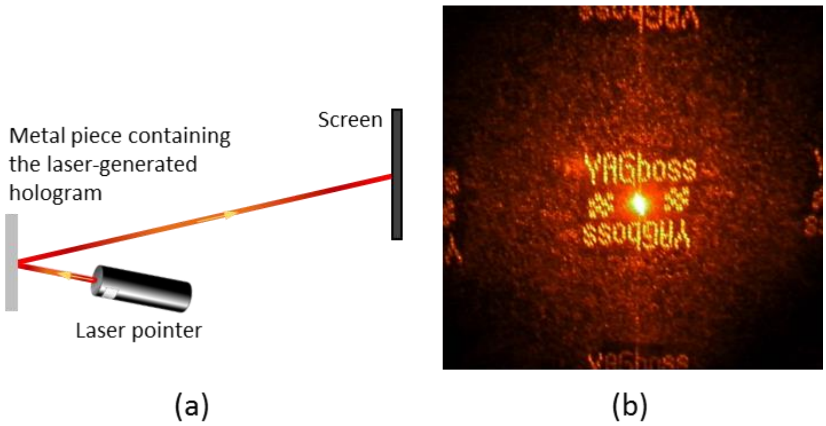

Figure 9. (a) Optical setup used for determining the optical performance of the laser-generated holograms and (b) an example of the diffractive image produced by the laser-generated hologram.

5. CONCLUSIONS

The paper described a novel laser-based approach for the generation of unique, optically-smooth, phase holographic structures directly on the surface of metals, such as stainless steel, nickel and nickel-chromium Inconel® alloys. The optical smoothness was obtained by using nanosecond laser pulses of wavelength 355nm. The holograms are robust to local damage and tamperproof. Therefore, they can be used as security markings for high-value metal products and components.

ACKNOWLEDGEMENTS

The research covered in this paper was funded by the Engineering and Physical Sciences Research Council (EPSRC): Centre for Innovative Manufacturing in Lased-based Production Processes (Grant No: EP/K030884/1), and Renishaw plc. (UK). Also the author would like to thank SISMA SpA (Italy) for provision of silver samples.

REFERENCES

[1] Wlodarczyk, K.L., Mendez, E., Baker, H.J., McBride, R., Hall, D.R., "Laser smoothing of binary gratings and multilevel etched structures in fused silica," Appl. Opt. 49, pp. 1997-2005 (2010).

[2] Von Allmen, M. and Blatter, A, [Laser-beam interactions with materials: physical principles and applications], Springer Verlag, (1995).

[3] Wissenbach, K., Weisheit, A., Willenborg, E, Temmler, A., Backes, G., Gasser, A., Gottman, J., "Surface treatment," in [Tailored light 2 – Laser application technology], R. Poprawe, ed., Springer RWTHedition, pp. 173-239 (2011).

[4] Hibiya, T and Ozawa, S., "Marangoni flow and surface tension of high temperature melts", in [High-temperature measurements of materials], H. Fukuyama and Y. Waseda, eds., Springer Berlin Heidelberg, pp. 39-57 (2009).

[5] Weston, N.J., Hand, D.P., Giet, S., Ardron, M. "A method of forming an optical device," Patent No.: WO/2012/ 038707 (2012).

[6] Goodman, J.W., [Introduction to Fourier Optics], Roberts & Company – Englewood, (2005).

[7] Wlodarczyk, K.L., Ardron, M., Waddie, A.J., Dunn, A., Kidd, M.D., Weston, N.J., Hand, D.P., "Laser micro-sculpting for the generation of robust diffractive security markings on the surface of metals," J. Mater. Process. Technol. 222, pp. 206-218 (2015).

[8] Freese, W., Kampfe, T., Kley, E.B., Tunnermann, A., "Design of binary subwave-length multiphase level computer generated holograms," Opt. Lett. 35, pp. 676–678 (2010).